Effects of mixture distribution on localised forced ignition of stratified mixtures: A Numerical Investigation

Dipal Patel, Nilanjan Chakraborty
School of Mechacnical and System Engineering, Newcastle University,
Newcastle Upon Tyne, NE1 7RU, UK

1 Introduction

Localised forced ignition (e.g. spark or laser ignition) of inhomogeneous mixtures has a number of important applications ranging from Gasoline Direct Injection (GDI) engines to Lean Premixed Prevaporised (LPP) combustors. A number of previous analyses concentrated on localised ignition of inhomogeneous mixtures where the mixture inhomogeneity is characterized by a gradient of mean equivalence ratio [1]. By contrast, localised forced ignition of stratified mixtures characterized by a constant global mean value of equivalence ratio $\langle\phi\rangle$ with a non-zero value of root-mean-square (rms) ϕ' is rarely analysed [2,3]. Pera *et al.* [2] demonstrated based on two-dimensional detailed chemistry Direct Numerical Simulations (DNS) that mixture inhomogeneity significantly affects the extent of flame wrinkling. Recently, Patel and Chakraborty [3] demonstrated that the rms value of equivalence ratio ϕ' and the Taylor micro- scale of equivalence ratio fluctuations (i.e. $l_\phi = \sqrt{6\langle[\phi-\langle\phi\rangle]^2\rangle/\langle\nabla[\phi-\langle\phi\rangle]\cdot\nabla[\phi-\langle\phi\rangle]\rangle}$) [3,4], where the angle bracket indicates the global mean evaluated over the whole computational domain) have significant influences on the early stage of combustion following successful localised forced ignition of stratified mixtures [3]. However, the analysis by Patel and Chakraborty [3] was restricted to globally stoichiometric (i.e.$\langle\phi\rangle$=1.0) stratified mixtures for which the initial equivalence ratio distribution was assumed to follow a bi-modal probability density function (pdf). The effects of the initial equivalence ratio distribution (i.e. pdf of ϕ) for a given set of values of ϕ' and l_ϕ on localised forced ignition of both globally fuel-lean and stoichiometric (i.e. $\langle\phi\rangle$=0.8 and $\langle\phi\rangle$=1.0) mixtures are yet to be analysed in detail. Here, the effects of initial mixture distribution have been investigated for both Gaussian and bi-modal distributions of equivalence ratio for a given set of values of ϕ' and l_ϕ for $\langle\phi\rangle$=0.8 and $\langle\phi\rangle$=1.0 mixtures using three-dimensional Direct Numerical Simulation (DNS) data for different values of rms turbulent velocity u'.

2 Mathematical Background and Numerical Implementation

A modified single step chemical mechanism of the form $Fuel + s\cdot Oxidiser \rightarrow (1+s)\cdot Products$ [5] (where s indicates the mass of oxidiser consumed per unit mass of fuel consumption under stoichiometric conditions) has been considered here for the purpose of computational economy [6], which allowed for an extensive parametric analysis as carried out in this paper. The activation energy and heat of combustion are taken to be functions of ϕ following Tarrazo *et al.* [5] so that realistic ϕ dependence of unstrained laminar burning velocity $S_{b(\phi)}$ can be obtained. The equivalence ratio ϕ can be expressed in terms of mixture fraction $\xi = (Y_F - Y_O/s + Y_{O\infty}/s)/(Y_{F\infty} + Y_{O\infty}/s)$ and stoichiometric

Correspondence to: d.patel2@ncl.ac.uk

mixture fraction $\xi_{st} = Y_{O\infty}/(sY_{F\infty} + Y_{O\infty})$ as $\phi = [1 - \xi_{st}]\xi/[1 - \xi]\xi_{st}$ where $Y_{F\infty}$ and $Y_{O\infty}$ are the fuel and oxidizer mass fractions in pure fuel and air stream respectively, and Y_F and Y_O are the local fuel and oxidizer mass fractions respectively. For the present analysis, $s = 4$; $Y_{F\infty} = 1.0$ and $Y_{O\infty} = 0.233$ have been taken, which yield $\xi_{st} = 0.055$, representative of methane-air binary mixture. The extent of the completion of the chemical reaction is quantified here with the help of a reaction progress variable $c = (\xi Y_{F\infty} - Y_F)/(\xi Y_{F\infty} - \max[0, (\xi - \xi_{st})/(1 - \xi_{st})]Y_{F\infty})$ [3,7] which rises from 0 in the fully unburned reactants to 1.0 in the fully burned products.

Table 1:Initial values of the simulation parameters for $\phi' = 0.2$[††]

	Globally fuel-lean stratified mixtures $\langle\phi\rangle = 0.8$ [L]		
$L_{11}/l_f = 3.36$	$u'/S_{b(\phi=1)} = 0.0$ [T0]	$u'/S_{b(\phi=1)} = 4.0$ [T4]	$u'/S_{b(\phi=1)} = 6.0$ [T6]
$l_\phi/l_f = 2.1$ [D]	LGXT0D; LBXT0D	LGXT4D; LBXT4D	LGXT6D; LBXT6D
$l_\phi/l_f = 5.5$ [E]	LGXT0E; LBXT0E	LGXT4E; LBXT4E	LGXT6E; LBXT6E
$l_\phi/l_f = 8.3$ [F]	LGXT0F; LBXT0F	LGXT4F; LBXT4F	LGXT6F; LBXT6F

The localised ignition is modelled by using a source term q''' in the energy transport equation, which deposits energy in the radial direction from the centre of the ignitor in the following manner [3,7,8]: $q'''(r) = A_q \exp(-r^2/2R^2)$ where r is the radial direction from the centre of the ignitor and R is the characteristic width of energy deposition, which is taken to be $R = 1.55 l_f$ for the present analysis where $l_f = D_0/S_{b(\phi=1)}$ is the Zel'dovich flame thickness of the stoichiometric mixture with D_0 and $S_{b(\phi=1)}$ being the unburned gas diffusivity and the unstrained laminar burning velocity of the stoichiometric mixture respectively. The constant A_q is determined by $\dot{Q} = \int_V q''' dV$ where the ignition power, $\dot{Q}$ is defined as: $\dot{Q} = a_{sp}\rho_0 C_P \tau T_0 (\{4/3\}\pi l_f^3)[\{H(t) - H(t - t_{sp})\}/t_{sp}]$ where $\tau = (T_{ad(\phi=1)} - T_0)/T_0$ is the heat release parameter with T_0 and $T_{ad(\phi=1)}$ being the initial reactant temperature and the adiabatic flame temperature of the stoichiometric mixture respectively, a_{sp} is a parameter which determines the total energy deposited by the ignitor and the Heaviside functions $H(t)$ and $H(t - t_{sp})$ ensure that the ignition source term q''' remains operational for the energy deposition duration t_{sp}. For the present analysis $a_{sp} = 9.2$ and $\tau = 3.0$ are taken and the Lewis number of all species is taken to be unity. The energy deposition duration t_{sp} is expressed as: $t_{sp} = b_{sp} t_f$ where b_{sp} is the energy deposition duration parameter and t_f is a characteristic chemical time scale given by $t_f = l_f/S_{b(\phi=1)}$. The parameter b_{sp} is taken to be 0.2 following previous analyses [3,8]. The ignitor centre is placed at the centre of the domain. The ignition model used here only addresses the thermal aspect of the localised forced ignition and the details of the spark formation (momentum modification contribution, plasma formation and shock wave) are kept beyond the scope of the present analysis in order to keep this study computationally feasible. The pseudo-spectral methods proposed by Eswaran and Pope [4] and Rogallo [9] were used for generating initial ϕ distribution following bi-modal and Gaussian distributions respectively. The initial values of normalised turbulent velocity fluctuation $u'/S_{b(\phi=1)}$, normalised longitudinal integral length scale L_{11}/l_f, rms of equivalence ratio ϕ' and normalised Taylor micro-scale of equivalence ratio variation l_ϕ/l_f are listed in Table 1. A compressible three-dimensional DNS code SENGA [7] was used to carry out the simulations under decaying turbulence in a domain of size $33l_f \times 33l_f \times 33l_f$, which is discretised by a Cartesian grid of size $200 \times 200 \times 200$ with uniform grid spacing ensuring 10 grid points within $\delta_{th(\phi=1)} = [T_{ad(\phi=1)} - T_0]/\mathrm{Max}|\nabla\hat{T}|_L$ where $\hat{T}$ is the instantaneous temperature. The boundaries in the $x_1 -$ direction are taken to be partially non-reflecting, whereas the boundaries in the other directions are considered to be periodic.

[††] Replace [X] with [Y] and [Z] for $\phi' = 0.4$ and 0.6. Replace [L] with [S] for $\langle\phi\rangle = 1.0$ where [G]: Gaussian distribution and [B]: Bi-modal distribution

3 Results and Discussion

The temporal evolution of the non-dimensional maximum temperature (i.e. $T_{\max} = (\hat{T}_{\max} - T_0)/(T_{ad(\phi=1)} - T_0)$) for all the simulation parameters considered in this study (see Table 1) are shown in Fig. 1, which shows that $T_{\max}$ rises with time until $t = 1.0t_{sp}$ due to energy deposition during $0 < t < t_{sp}$. The non-dimensional maximum temperature $T_{\max}$ settles to $T \approx 1.0$ at $t \gg t_{sp}$ in the cases where self-sustained combustion is obtained following successful ignition. Figure 1 shows that self-sustained combustion has been obtained for all cases with $\langle\phi\rangle = 1.0$ where some cases with $\langle\phi\rangle = 0.8$ cases fail to achieve self sustained combustion. It is found that the initial Gaussian distribution cases with $\langle\phi\rangle = 0.8$ and $u'/S_{b(\phi=1)} = 6.0$ show flame extinction at $t \gg t_{sp}$ irrespective values of ϕ' but the cases with initial bi-modal distribution for $\langle\phi\rangle = 0.8$ with initial values of $\phi' = 0.2$; $l_\phi/l_f = 5.5$(i.e. LBXT6E), $\phi' = 0.4$; $l_\phi/l_f = 8.3$ (i.e. LBYT6F) and $\phi' = 0.6$; $l_\phi/l_f = 8.3$ (i.e. LBZT6F) with $u'/S_{b(\phi=1)} = 6.0$ show self-sustained combustion at $t \gg t_{sp}$. Additionally Fig. 1 shows that all cases for initial Gaussian distribution with $u'/S_{b(\phi=1)} = 4.0$ achieve self-sustaiend combsutiuon following successful ignition, whereas the bi-modal distribution cases LBYT4E and LBZT4E with initial $u'/S_{b(\phi=1)} = 4.0$ exhibit flame extinction at $t \gg t_{sp}$. However, the probability of flame extinction at $t > t_{sp}$ increases with increasing $u'/S_{b(\phi=1)}$ for $\langle\phi\rangle = 0.8$ in both bi-modal and Gaussian distribution cases. Figure 1 suggests that the influence of initial mixture inhomogeneity distribution, $u'/S_{b(\phi=1)}$, ϕ' and l_ϕ/l_f have important influences on the possibility of obtaining self-sustained combustion following successful ignition in stratified mixtures. The contours of ϕ, $T = (\hat{T} - T_0)/(T_{ad(\phi=1)} - T_0)$, Y_F and. $|\dot{w}_F|$ for the cases considered here are qualitatively similar to the distributions shown in Ref. [3] and thus are not shown here.

The evolution of mixing process can be illustrated by the temporal evolution of the pdfs of ϕ, which is shown in Fig. 2 for the selected $\langle\phi\rangle = 0.8$ cases. For the initial Gaussian distribution cases, there is a higher probability of finding $\phi \approx \langle\phi\rangle = 0.8$ than in the initial bi-modal distribution cases. The equivalence ratio pdfs for the initial Gaussian distribution show peak values at $\phi \approx \langle\phi\rangle = 0.8$, whereas the cases with initial bi-modal distribution show higher probabilities of finding $\phi < \langle\phi\rangle$ and $\phi > \langle\phi\rangle$ than the initial Gaussian distribution cases. It can be seen from Fig. 2 that the pdf of ϕ for the initial bi-modal distribution cases approaches an approximate Gaussian distribution as time progresses due to mixing, whereas the width of ϕ pdf decreases, and the peak value of ϕ pdf at $\phi \approx \langle\phi\rangle = 0.8$ increases with time for the initial Gaussian distribution cases. Figure 2 demonstrates that the effect of mixing are greater for smaller values of l_ϕ/l_f for a given value of $u'/S_{b(\phi=1)}$, as the mean scalar dissipation rate of mixture fraction $N_\xi = D\nabla\xi \cdot \nabla\xi$ scales as $\langle N_\xi\rangle \sim D\xi'^2/l_\phi^2$ where ξ' is the rms value of mixture fraction induced by equivalence ratio fluctuations. This suggests that N_ξ is likely assume higher magnitudes for smaller values of l_ϕ/l_f for a given value of ξ'. Furthermore the probability of finding high values of N_ξ increases with increasing $u'/S_{b(\phi=1)}$ as turbulent staining acts to generate scalar gradient which in turn increases the rate of micro-mixing. The temporal evolution of ϕ pdf and the influences of u' and l_ϕ on N_ξ and micro-mixing in the globally stoichiometric mixtures (i.e. $\langle\phi\rangle = 1.0$) are found to be qualitatively similar to $\langle\phi\rangle = 0.8$ mixtures shown in Fig. 2 and thus are not explicitly shown here.

The percentage of overall heat release arising from premixed (i.e. $I_c > 0$) and non-premixed (i.e. $I_c < 0$) modes of combustion for selected cases at $t = 8.40t_{sp}$ are shown in Fig. 3 where $I_c = \nabla Y_F \cdot \nabla Y_O/(|\nabla Y_F||\nabla Y_O|)$ is the flame index, which assumes positive (negative) values for premixed (non-premixed) mode of combustion. It is evident from Fig. 3 that the chemical reaction takes place predominantly in premixed mode but some pockets of non-premixed combustion can also be found. Figure 3 shows that the percentage of heat release from the premixed mode of combustion is greater in the initial Gaussian mixture distribution in comparison to the initial bi-modal distribution. This is consistent with higher probability of finding $\phi \approx \langle\phi\rangle$ in the Gaussian mixture distribution than in the case of bi-modal distribution as shown in Fig. 2. The percentage of heat release arising from the non-premixed mode of combustion increases with increasing ϕ' for both types of initial mixture distributions, but this effect is more prominent in the initial bi-modal distribution cases than the initial Gaussian distribution cases. Furthermore, the percentage of heat release with $I_c < 0$ decreases with decreasing values of l_ϕ/l_f for a given value of ϕ' as a result of improved mixing due to high magnitudes of N_ξ (not shown here).

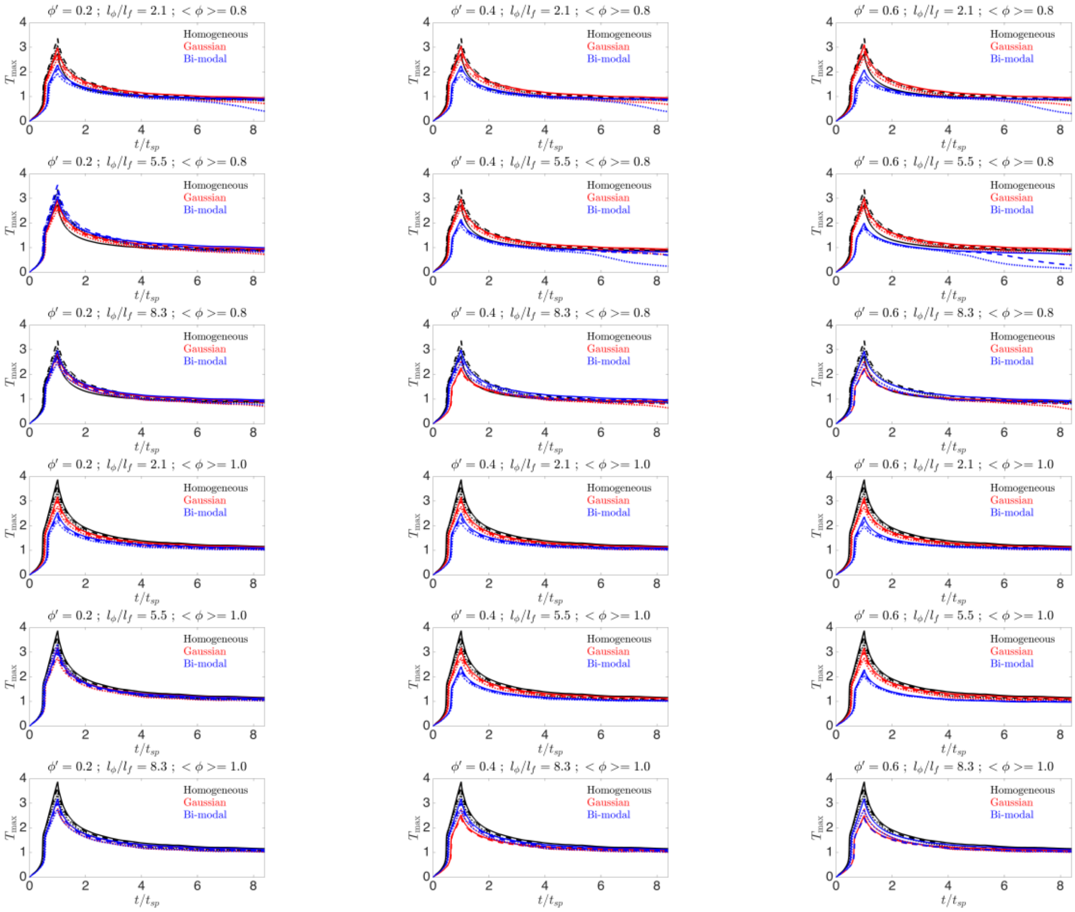

Figure 1: Temporal evolution of the maximum values of non-dimensional temperature for all cases listed in Table 1 ($u'/S_{b(\phi=1)}$ =0.0 :———, $u'/S_{b(\phi=1)}$=4.0: — — —; $u'/S_{b(\phi=1)}$=6.0: - - - - -).

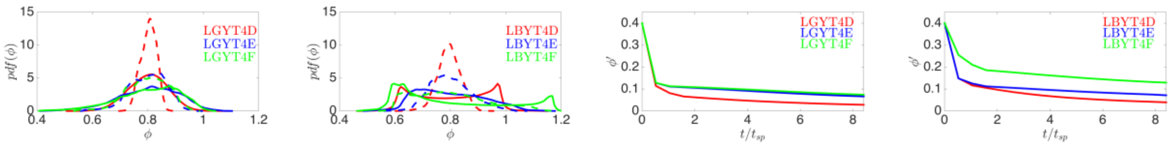

Figure 2: Temporal evolution of (a) the pdf of ϕ at $t = 1.05t_{sp}$ (solid line) and $t = 8.40t_{sp}$ (broken line) and (b) ϕ' evaluated over the whole domain for the selected cases.

The extent of burning can be characterised by the mass of burned gas M_b with $c \geq 0.9$ [3,7]. The temporal evolution of the normalised value of M_b for all cases considered in this study are shown in Fig. 4. It is evident from Fig. 4 that M_b decreases for higher values of $u'/S_{b(\phi=1)}$ in both initial bi-modal and Gaussian distributions of ϕ. An increase in u' leads to an increase in eddy diffusivity $D_t \sim u'L_{11}$ for a given value of L_{11}, which leads to greater amount of heat loss from the hot gas kernel for high values of $u'/S_{b(\phi=1)}$. Additionally Fig. 4 shows that in increase in ϕ' leads to a decrease of M_b for all cases irrespective of initial mixture distributions and the value of $\langle\phi\rangle$. The laminar burning velocity $S_{b(\phi)}$ of mixtures with $\phi < 1.0$ and $\phi > 1.10$ is smaller than that in the mixtures with $1.0 \leq \phi \leq 1.10$. The probability of finding $1.0 \leq \phi \leq 1.10$ decreases with increasing ϕ' and this gives rise to a reduction in burning rate for high values of ϕ'. The probability of finding highly reactive mixture corresponding to

$1.10 > \phi > 1.0$ is greater in the cases with $\langle \phi \rangle = 1.0$ in comparison to those with $\langle \phi \rangle = 0.8$, thus M_b attains higher value for the $\langle \phi \rangle = 1.0$ cases than in the $\langle \phi \rangle = 0.8$ cases. Figure 4 further shows that M_b remains comparable for the quiescent cases with initial values of $\phi' = 0.2$ for all values of l_ϕ/l_f in both initial bi-modal and Gaussian distributions. Among the bi-modal cases with initial ϕ'=0.2, the burned gas mass assumes the highest (lowest) values for the cases with initial $l_\phi/l_f = 5.5$ ($l_\phi/l_f = 2.1$). However, the burned gas mass assumes the highest (lowest) values for the cases with initial $l_\phi/l_f = 8.3$ ($l_\phi/l_f = 5.5$) for initial ϕ'=0.4 and 0.6 in the bi-modal distribution cases. By contrast, the initial Gaussian mixture distribution cases show an increase in burned gas mass with decreasing values of l_ϕ/l_f irrespective of the value of ϕ', as the probability of finding $1.0 \leq \phi \leq 1.10$ ($0.8 \leq \phi \leq 1.10$) mixtures in the $\langle \phi \rangle = 1.0$ ($\langle \phi \rangle = 0.8$) cases increases with decreasing l_ϕ/l_f due more efficient mixing for smaller values of l_ϕ.

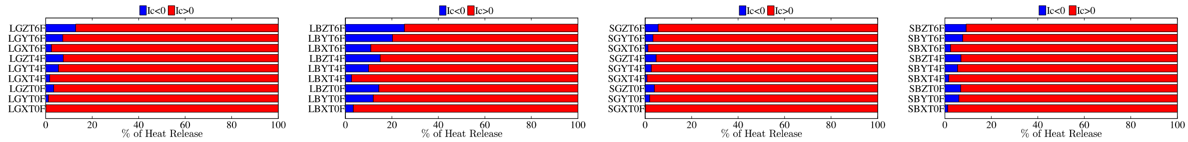

Figure 3: Percentage of overall heat release arising from premixed ($I_c > 0$) and non-premixed ($I_c < 0$) combustion at $t = 8.40t_{sp}$ for selected cases.

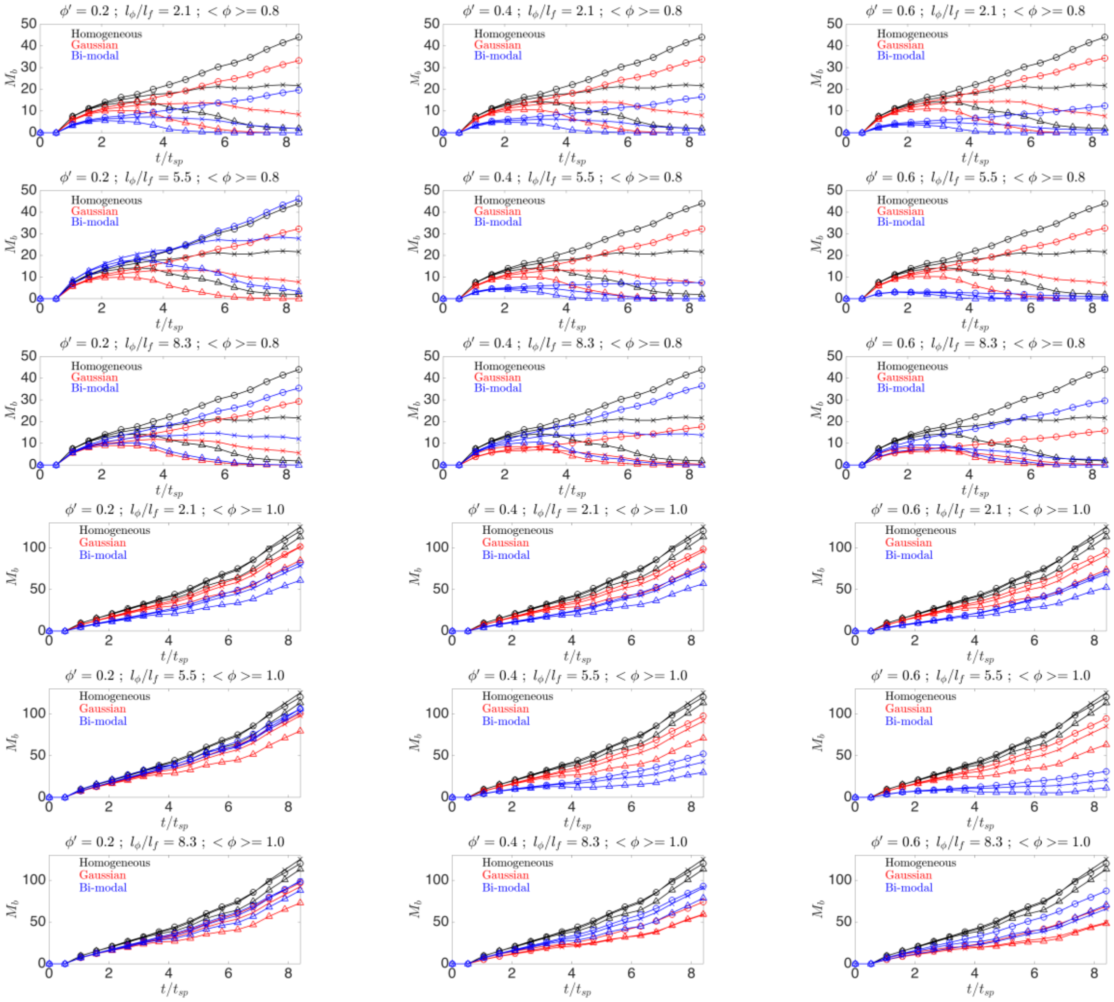

Figure 4: Temporal evolution of $M_b = [m_b(c \geq 0.9)]/[\{4/3\}\pi\rho_0 l_f^3]$ for all cases listed in Table 1 (with $u'/S_{b(\phi=1)}$ = 0.0 [O], 4.0 [X] and 6.0 [△]).

The probability of finding mixtures corresponding to $1.10 \geq \phi \geq 1.0$ ($1.10 \geq \phi \geq 0.8$) is greater in the $\langle\phi\rangle = 1.0$ ($\langle\phi\rangle = 0.8$) cases with initial values of $l_\phi/l_f = 5.5$ and 8.3 than in the initial $l_\phi/l_f = 2.1$ cases due to less efficient mixing for the initial bi-modal distribution cases with ϕ'=0.2. This gives rise to greater rate of burning in the bi-modal distribution cases with initial values of $l_\phi/l_f = 5.5$ and 8.3 than in the initial $l_\phi/l_f = 2.1$ cases for initial values of ϕ'=0.2. The probability of finding more reactive $1.0 \leq \phi \leq 1.10$ ($0.8 \leq \phi \leq 1.10$) mixture is smaller for initial $l_\phi/l_f = 5.5$ cases than the initial $l_\phi/l_f = 2.1$ cases for bi-modal distribution with initial values of $\phi' = 0.4$ and 0.6. This gives rise to smaller burned gas mass for initial $l_\phi/l_f = 5.5$ cases than the initial $l_\phi/l_f = 2.1$ cases for bi-modal distribution. For bi-modal cases with initial $l_\phi/l_f = 8.3$ the clouds of mixture inhomogeneities are relatively big, and as a result, there is a high probability of obtaining a large region of almost homogeneous mixture at the centre of ignitor. If the ignitor centre is located in the vicinity of a large cloud of $1.0 \leq \phi \leq 1.1$ ($0.8 \leq \phi \leq 1.10$) in the $\langle\phi\rangle = 1.0$ ($\langle\phi\rangle = 0.8$) case, the slow burning rate in the pockets with $1.0 < \phi$ ($0.8 < \phi$) and $\phi > 1.10$ encountered during the expansion of hot gas kernel is mostly compensated by the high burning rate in the $1.0 \leq \phi \leq 1.1$ ($0.8 \leq \phi \leq 1.10$) mixture and this leads to greater burned gas mass in the cases with initial $l_\phi/l_f = 8.3$ than in the cases with initial $l_\phi/l_f = 2.1$ when the initial ϕ' is either 0.4 or 0.6 for the initial bi-modal distribution.

4 Conclusions

The effects of l_ϕ/l_f, ϕ' and $u'/S_{b(\phi=1)}$ on localised forced ignition of $\langle\phi\rangle = 0.8$ and 1.0 stratified mixtures have been numerically investigated for both initially Gaussian and bi-modal distributions of ϕ. For a given value of l_ϕ/l_f, an increase in ϕ' leads to a reduction of burned gas mass for both Gaussian and bi-modal distributions, whereas the influence of l_ϕ/l_f on the extent of burning has been found to be non-monotonic and dependent on ϕ' for the initial bi-modal mixture distribution, whereas the initial Gaussian mixture distribution shows an increase in burned gas mass with decreasing values of l_ϕ/l_f irrespective of ϕ' and $\langle\phi\rangle$ considered here. The increase in heat transfer rate from hot gas kernel with an increase in $u'/S_{b(\phi=1)}$ leads to a decrease in the extent of burning. The above findings demonstrate that favorable conditions in terms of initial distribution of ϕ, $\langle\phi\rangle$ l_ϕ/l_f, ϕ' and u' are required for self-sustained combustion following successful ignition of stratified mixtures.

References

[1] Mastorakos, E. (2009). Ignition of non-premixed flames, Prog. Energy Combust. Sci., 35:57.
[2] Pera, C., Chevillard, S., Reveillon, J. (2010). Effect of residual burnt gas heteroneneity on early flame propagation and on cyclic variability in spark-ignited engines, Combust. Flame, 160:1020.
[3] Patel, D., Chakraborty, N. (2014). Localised forced ignition of globally stoichiometric stratified mixtures: A Numerical Investigation, Combust. Theo. Mod., 18:627.
[4] Eswaran V, Pope SB. (1988). Direct Numerical Simulations of the turbulent mixing of a passive scalar, Phys. Fluids, 31:506.
[5] Tarrazo E, Sanchez A, Liñán A, Williams FA. (2006). A simple one-step chemistry model for partially premixed hydrocarbon combustion, Combust. Flame, 147:32.
[6] Chen, J.H. et al. (2009). Terascale direct numerical simulations of turbulent combustion using S3D, Comput. Sci. & Discovery, Paper no. 015001
[7] Chakraborty, N., Mastorakos, E., Cant, R.S. (2007). Effects of turbulence on spark ignition in inhomogeneous mixtures: A direct numerical simulation (DNS) study, Combust. Sci. Tech., 179: 293.
[8] Espi, C.V., Liñán, A. (2001). Fast, non-diffusive ignition of a gaseous reacting mixture subject to a point energy source, Combust. Theo. Mod., 5:485.
[9] Rogallo, R.S. (1981). Numerical experiments in homogeneous turbulence. NASA Technical Memorandum 81315. California.